8th IEEE Conference on Mechatrinics and Machine Vision in Practice
Hong Kong 2001

Wavelet-based Detection of Local Textile Defects

Grantham Pang, Ajay Kumar
Industrial Automation Research Laboratory
Department of Electrical & Electronic Engineering
The University of Hong Kong
Hong Kong
Email: gpang@eee.hku.hk
http://ial.eee.hku.hk

***Abstract*-- In this paper, the problem of fabric defect detection using machine vision is investigated. Every inspection image is used to generate two projection signals along the horizontal and vertical planes respectively. Each of these signals is then normalized to have zero mean and unity variance. Wavelet decomposition of these normalized projection signals is used to enhance defect information. A simple thresholding operation on these wavelet coefficients extracts the defects and their localization. Experimental results presented in this paper show that this approach is highly successful in detecting variety of fabric defects and, can provide low-cost, single PC-based, solution to the web inspection problem.**

***Index terms*-- Quality Assurance, Defect Detection, Computer Vision, Wavelet Analysis, Industrial Automation.**

I. INTRODUCTION

Machine-vision based inspection of industrial products offers low cost, high speed and high quality of defect detection. Many researchers have investigated the problem of fabric defect detection using various approaches [1]-[3]. Details on these approaches can be found in [4]. Low-cost, PC-based, web inspection systems are in increasing demand. This paper describes a low-cost approach for the inspection of textile web using wavelet transform. Wavelet analysis has become a common tool for analyzing localized variations of power within a signal. Kim et al. [3] have presented a wavelet-based approach for the detection of fabric defects. The novel aspects of the approach presented in this paper is its simplicity and success in the detection of variety of fabric defects. In addition, the approach presented in this paper not only detects the presence of defects, but also determines their approximate localization on the web. The information about the location of defects is very useful in generating inspection report and helps to take corrective measures.

II. METHODOLOGY

The block diagram of the proposed defect detection method is shown in figure 1. Two projection signals, $s'_h(n)$ and $s'_v(m)$, are generated from the vibration-free inspection image $I(m,n)$ of size $M \times N$ pixels. These signals are generated by addition of gray-level pixel values along the rows and columns respectively.

$$\begin{aligned} s'_h(n) &= \sum_{m=1}^{M} I(m,n), \\ s_h(n) &= \frac{1}{\sigma_h}\{s'_h(n) - \mu_h\}, \\ s'_v(m) &= \sum_{n=1}^{N} I(m,n), \\ s_v(m) &= \frac{1}{\sigma_v}\{s'_v(m) - \mu_v\} \end{aligned} \tag{1}$$

where the μ_h and μ_v are the mean values of signal $s'_h(n)$ and $s'_v(m)$ respectively, and are used to make $s_h(n)$ and $s_v(m)$ zero mean. Similarly, σ_h and σ_v are the variance of signal $s'_h(n)$ and $s'_v(m)$ respectively, and are used to make $s_h(n)$ and $s_v(m)$ of unity variance.

The wavelet decomposition of these 1-D signals is used to enhance the defect information. The choice of wavelet bases is arbitrary, as is with the several other traditional transforms, *e.g.* Fourier, Lagendre, *etc*.. The factors affecting the selection of wavelet bases and their parameters has been discussed in [5]. Morlet wavelet, which consists of a plane wave modulated by a Gaussian, is used in the work. This wavelet function (figure 2) can be written as:

$$Z(t) = \exp(j\omega_0 t)\exp(-t^2/2) \tag{2}$$

where ω_0 is the nondimensional frequency, taken here to be 6 to satisfy the admissibility condition [5]. The continuous wavelet transform of a discrete projection signal $s_h(n)$ is defined as the convolution of $s_h(n)$ with the scaled and translated version of $Z(t)$:

$$W_s^h(n) = \sum_{k=0}^{N-1} s_h(k) Z^* \left\{ \frac{(k-n)}{s} \right\} \qquad (3)$$

where the (*) indicates the complex conjugate, *s* the *scale*, and *n* is the localized time or spatial index. The length of wavelet function was empirically fixed, with the objective of minimizing computational time and achieving the robust results. A 32 point Morlet wavelet function at $s = 8$ is used for all the experiments performed and reported in this paper.

The wavelet decomposed signals $W_s^h(n)$ and $W_s^v(m)$, corresponding to signals $s_h(n)$ and $s_v(m)$ respectively, are obtained for a given scale. Due to the finite-length of the signals $s_h(n)$ (1×640) and $s_v(m)$ (1×480), errors will occur at the beginning and at the end of signals $W_s^h(n)$ and $W_s^v(m)$. Several solutions to limit these errors, such as zero padding, cosine damping, *etc*., have been detailed in [6]. For the reasons of computational simplicity, discontinuities due to edge effect in this work are avoided by discarding (padding with zeros) 32 points at the beginning and at the end of signals $W_s^h(n)$ and $W_s^v(m)$. The absolute magnitude of these signals are subjected to the thresholding operation, and the thresholded signal shows the position of defect (if any) in the image under inspection.

The thresholding limits t_1 and t_2 is determined from a defect-free (reference) fabric sample before the beginning of inspection. This reference fabric is used to compute the projection signals $s_{h_{ref}}(n)$ and $s_{v_{ref}}(m)$ using equation (1). These signals are used to compute the decomposed signals $W_s^{h_{ref}}(n)$ and $W_s^{v_{ref}}(m)$ using equation (3). The thresholding limit t_1 and t_2, for the horizontal and vertical projection signals respectively, is determined as follows [4]:

$$t_1 = \max_{n \in K} |W_s^{h_{ref}}(n)|, \quad t_2 = \max_{m \in K} |W_s^{v_{ref}}(m)| \qquad (4)$$

where '*K*' is the window at the center of the signal. This window is used to limit the edge distortion (as discussed earlier), and its size in this work is obtained by ignoring 32 points from each side of signals $W_s^{h_{ref}}(n)$ and $W_s^{v_{ref}}(m)$.

III. Experimental Setup and Results

Several real fabric samples were collected from the textile industry and used to evaluate the performance of the proposed defect detection scheme. In all experiments, low-resolution fabric sample images of about 45 pixels per inches are used. The low-resolution images can capture larger area of fabric per frame, which results in increased throughput. Using an Ominivision digital OV7110 camera with 640 × 480 pixels, vibration-free BW images of fabric samples under inspection were acquired. The experimental results with these fabric samples were excellent and are summarized in table 1. The first two entries of this table are reproduced in this paper and shown in figure 3 and figure 4.

IV. Conclusions

The defect detection scheme proposed in this paper is quite successful in detection of fabric defects from the low-resolution images. Due to the normalization of projection signals, the thresholding limit suggested in equation (4) has been found to be robust in detecting defects and suppressing noise. The proposed declaration of defects by thresholding of wavelet coefficients offer higher computational savings as compared to the case when the defects are declared by using Signal to Noise Ratio (SNR) as in [3]. The non-uniform illumination of the inspection images has not generated any problem in the detection of fabric defects. Thus the proposed defect detection scheme can be used to provide a low-cost, single PC-based, solution to the web inspection problem.

V. References

[1] A. Kumar and G. Pang, "Fabric defect segmentation using multi-channel blob detectors," Opt. Eng., vol. 39, no. 12, pp. 3176-3190, Dec. 2000.

[2] C. H. Chan and G. Pang, "Fabric defect detection by Fourier analysis," IEEE Trans. Ind. Appl., vol. 36, pp. 1267-1276, Sep/Oct. 2000.

[3] S. Kim, M. H. Lee, and K.B. Woo, "Wavelet Analysis to defects detection in weaving processes," in Proc. IEEE Int. Symp. Industrial Electronics, vol. 3, pp. 1406-1409, July 1998.

[4] Ajay Kumar, Automated defect detection in textured materials, Ph.D. Thesis, Department of Electrical and Electronic Engineering, The University of Hong Kong, Hong Kong, May 2001.

[5] M. Farge, "Wavelet transforms and their applications to turbulence," Annu. Rev. Fluid Mech., vol. 24, pp. 395-457, 1992.

[6] S. D. Mayers, B. G. Kelly, and J. J. O'Brein, "An introduction to wavelet analysis in oceanography and meteorology: With applications to the dispersion of Yanai waves," Mon. Wea. Rev., vol. 121, pp. 2858-2866, 1993.

Table1: Summary of fabric defect detection results.

S.No.	Name of the defect	Result from Horizontal projection	Results from vertical projection	Comments
1.	*Netting-multiplies*	Full detection	No detection	Figure 3
2.	*Shuttle-mark* (1)	Full detection	Full detection	Figure 4
3.	*Dirty-yarn*	Full detection	No detection	
4.	*Thick-yarn* (1)	No detection	Full detection	
5.	*Mispick*	No detection	Full detection	
6.	*Shuttle-mark* (2)	No detection	Full detection	
7.	*Wavy-face*	No detection	Full detection	
8.	*Wrong-draw*	No detection	Full detection	
9.	*Thin-bar*	No detection	Full detection	
10.	*Thick-yarn* (2)	Full detection	No detection	
11.	*Oil-stain*	No detection	Partial detection	Very small variation in the projection signals.
12.	*Break-out*	Detection with false alarm	No detection	False alarm, because of creases in the image.
13.	*Slack-end*	No detection	Full detection	

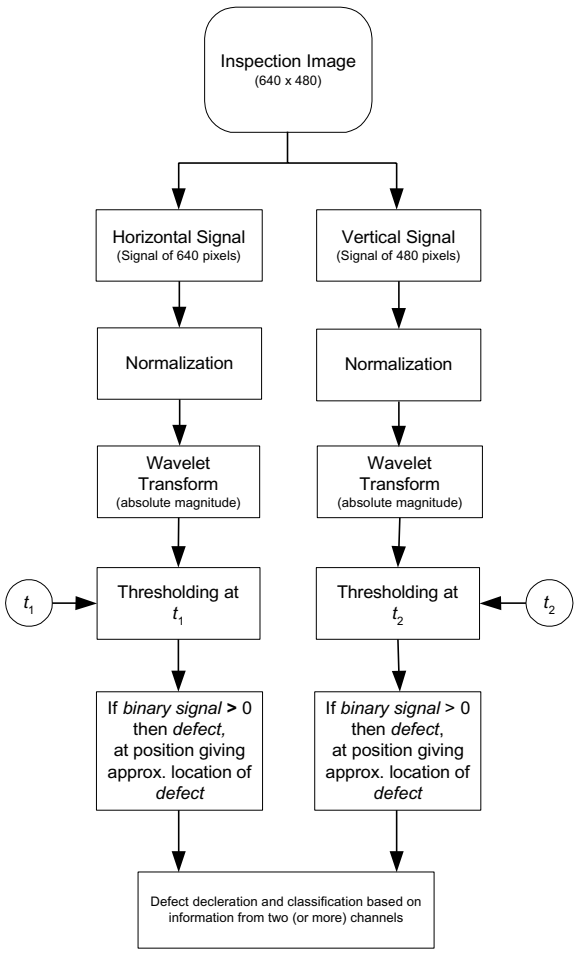

Figure 1: Block diagram for the wavelet-based defect detection scheme.

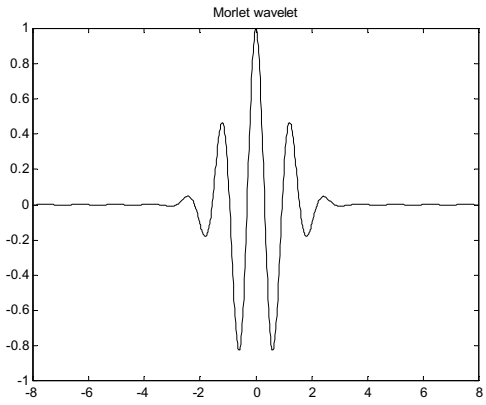

Figure 2: Morlet wavelet function.

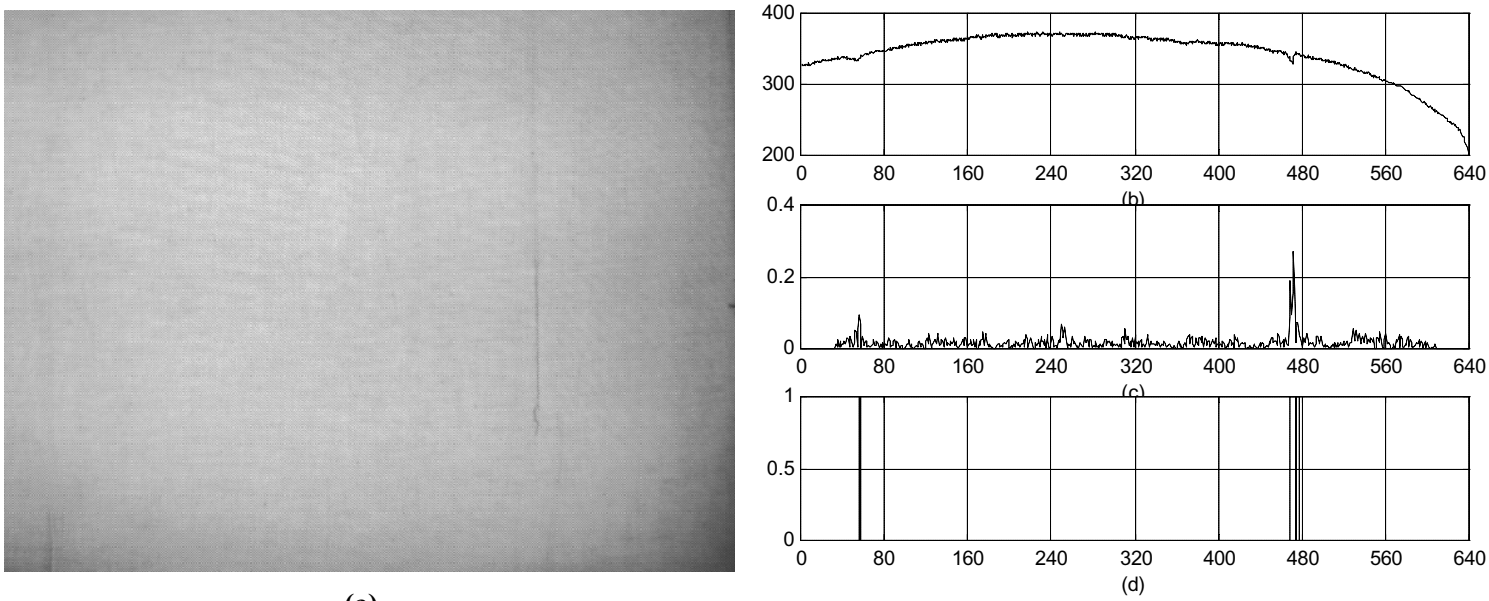

(a)

Figure 3: (a) Fabric sample with defect *netting-multiplies*, (b) horizontal projection signal $s'_h(n)$, (c) convolution with the wavelet function $|W_s^h(n)|$, (d) defects detected after thresholding.

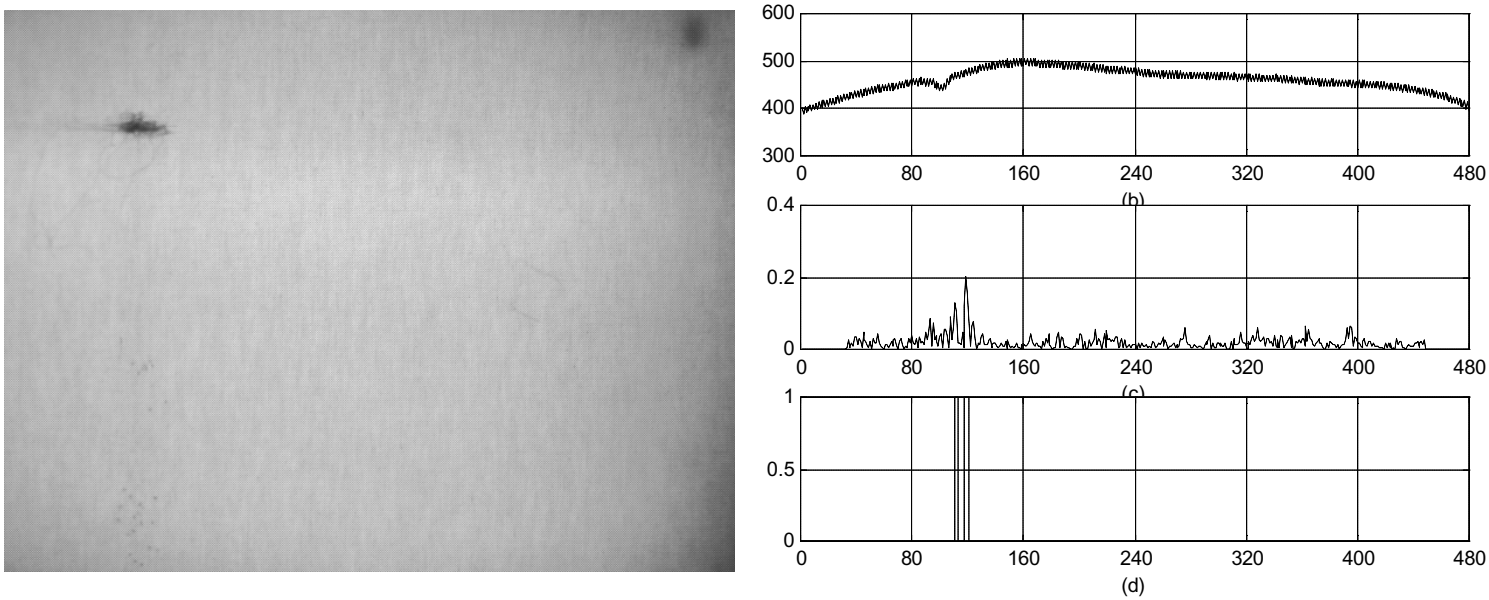

(a)

Figure 4: (a) Fabric sample with defect *shuttle-mark*, (b) Vertical projection signal $s'_v(m)$, (c) convolution with the wavelet function $|W_s^v(m)|$, (d) defects detected after thresholding.